J|A|C|S
ARTICLES
Published on Web 02/11/2006

2,7-Diphenyl[1]benzoselenopheno[3,2-*b*][1]benzoselenophene as a Stable Organic Semiconductor for a High-Performance Field-Effect Transistor

Kazuo Takimiya,*,† Yoshihito Kunugi,‡,¶ Yasushi Konda,† Hideaki Ebata,† Yuta Toyoshima,‡ and Tetsuo Otsubo†

Contribution from the Department of Applied Chemistry, Graduate School of Engineering, Hiroshima University, 1-4-1 Kagamiyama, Higashi-Hiroshima 739-8527, Japan, and Faculty of Integrated Arts and Sciences, Hiroshima University, 1-7-1 Kagamiyama, Higashi-Hiroshima 739-8521, Japan

Received November 9, 2005; E-mail: ktakimi@hiroshima-u.ac.jp

Abstract: [1]Benzoselenopheno[3,2-*b*][1]benzoselenophene (BSBS) and its 2,7-diphenyl derivative (DPh-BSBS) were readily synthesized from diphenylacetylene and bis(biphenyl-4-yl)acetylene, respectively, with a newly developed straightforward selenocyclization protocol. In contrast to the parent BSBS that has poor film-forming properties, the diphenyl derivative DPh-BSBS formed a good thin film on the Si/SiO_2 substrate by vapor deposition. X-ray diffraction examination revealed that this film consists of highly ordered molecules that are nearly perpendicular to the substrate, making it suitable for use in the fabrication of organic field-effect transistors (OFETs). When fabricated at different substrate temperatures (room temperature, 60 °C, and 100 °C) in a "top-contact" configuration, all the DPh-BSBS-based OFET devices exhibited excellent *p*-channel field-effect properties with hole mobilities >0.1 cm^2 V^{-1} s^{-1} and current on/off ratios of $\sim 10^6$. This high performance was essentially maintained over 3000 continuous scans between $V_g = +20$ and -100 V and reproduced even after storage under ambient laboratory conditions for at least one year.

Introduction

Organic field-effect transistors (OFETs) have attracted much attention as low-cost alternatives to conventional silicon-based transistors, and recent intensive research efforts in this field have led to the development of a number of superior *p*-channel organic semiconductors showing mobilities higher than 0.1 cm^2 V^{-1} s^{-1} in FET devices, almost comparable to that of amorphous silicon.[1−14] Showing remarkable properties are pentacene as the best thin-film material (0.3−0.7 cm^2 V^{-1} s^{-1} on a Si/SiO_2 substrate,[2] 1.5 cm^2 V^{-1} s^{-1} on a chemically modified Si/SiO_2 substrate,[3] and 3.0 cm^2 V^{-1} s^{-1} on a modified alumina substrate[4]) and rubrene as the best single-crystal material (∼20 cm^2 V^{-1} s^{-1}).[5] One of the remaining key challenges in the practical application of such OFETs is to enhance device durability. In this regard, considerable attention has been paid to the stability of organic semiconducting materials under ambient conditions.[7−13] The main reason for the low durability is sensitivity to air of the organic semiconducting materials used

† Graduate School of Engineering.
‡ Faculty of Integrated Arts and Sciences.
¶ Present address: Department of Applied Chemistry, Faculty of Engineering, Tokai University, 1117 Kitakaname, Hiratsuka 259-1292, Japan.

(1) (a) Dimitrakopoulos, C. D.; Malenfant, R. L. *Adv. Mater*. **2002**, *14*, 99−117. (b) Katz, H. E.; Bao, Z.; Gilat, S. L. *Acc. Chem. Res*. **2001**, *34*, 359−369. (c) Katz, H. E. *J. Mater. Chem*. **1997**, *7*, 369−376. (d) Rogers, J. A.; Bao, Z.; Katz, H. E.; Dodabalapur, A. In *Thin-Film Transistors*; Kagan, C. R., Andry, P., Eds.; Marcel Dekker: New York, 2003; p 377.
(2) Gundlach, D. J.; Lin, Y. Y.; Jackson, T. N.; Nelson, S. F.; Schlom, D. G. *IEEE Electron Device Lett.* **1997**, *18*, 87−89.
(3) Lin, Y. Y.; Gundlach, D. J.; Nelson, S. F.; Jackson, T. N. *IEEE Electron Device Lett.* **1997**, *18*, 606−608.
(4) Kelly, T. W.; Boardman, L. D.; Dunbar, T. D.; Muyres, D. V.; Pellerite, M. J.; Smith, T. P. *J. Phys. Chem. B* **2003**, *107*, 5877−5881.
(5) (a) Podzorov, V.; Pudalov, V. M.; Gershenson, M. E. *Appl. Phys. Lett.* **2003**, *82*, 1739−1741. (b) Podzorov, V.; Sysoev, S. E.; Loginova, E.; Pudalov, V. M.; Gershenson, M. E. *Appl. Phys. Lett.* **2003**, *83*, 3504−3506. (c) Sundar, V. C.; Zaumseil, J.; Podzorov, V.; Menard, E.; Willett, R. L.; Someya, T.; Gershenson, M. E.; Rogers, J. A. *Science* **2004**, *303*, 1644−1646. (d) Podzorov, V.; Menard, E.; Borissov, A.; Kiryukhin, V.; Rogers, J. A.; Gershenson, M. E. *Phys. Rev. Lett.* **2004**, *93*, 086602.
(6) (a) Katz, H. E. *Chem. Mater*. **2004**, *16*, 4748−4756. (b) Takimiya, K.; Kunugi, Y.; Toyoshima, Y.; Otsubo, T. *J. Am. Chem. Soc.* **2005**, *127*, 3605−3612. (c) Merlo, J. A.; Newman, C. R.; Gerlach, C. P.; Kelley, T. W.; Muyres, D. V.; Fritz, S. E.; Toney, M. F.; Frisbie, C. D. *J. Am. Chem. Soc.* **2005**, *127*, 3997−4009. (d) Payne, M. M.; Parkin, S. R.; Anthony, J. E.; Kuo, C.-C.; Jackson, T. N. *J. Am. Chem. Soc.* **2005**, *127*, 4986−4987. (e) Xiao, K.; Liu, Y.; Qi, T.; Zhang, W.; Wang, F.; Gao, J.; Qiu, W.; Ma, Y.; Cui, G.; Chen, S.; Zhan, X.; Yu, G.; Qin, J.; Hu, W.; Zhu, D. *J. Am. Chem. Soc.* **2005**, *127*, 13281−13286.
(7) Sirringhaus, H.; Wilson, R. J.; Friend, R. H. *Science* **1998**, *280*, 1741−1744.
(8) Li, W.; Katz, H. E.; Lovinger, A. J.; Laquindanum, L. G. *Chem. Mater*. **1999**, *11*, 458−465.
(9) Hong, X. M.; Katz, H. E.; Lovinger, A. J.; Wang, B.-C.; Raghavachari, K. *Chem. Mater*. **2001**, *13*, 4686−4691.
(10) (a) Ong, B. S.; Wu, Y.; Liu, P.; Gardner, S. *J. Am. Chem. Soc.* **2004**, *126*, 3378−3379. (b) Ong, B.; Wu, Y.; Jiang, L.; Liu, P.; Murti, K. *Synth. Met.* **2004**, *142*, 49−52. (c) Wu, Y.; Liu, P.; Gardner, S.; Ong, B. S. *Chem. Mater*. **2005**, *17*, 221−223.
(11) (a) Meng, H.; Bao, Z.; Lovinger, A. J.; Wang, B.-C.; Mujsce, A. M. *J. Am. Chem. Soc.* **2001**, *123*, 9214−9215. (b) Meng, H.; Zheng, J.; Lovinger, A. J.; Wang, B.-C.; Van Patten, P. G.; Bao, Z. *Chem. Mater*. **2003**, *15*, 1778−1787.
(12) (a) Wu, Y.; Li, Y.; Gardner, S.; Ong, B. S. *J. Am. Chem. Soc.* **2005**, *127*, 614−618. (b) Li, Y.; Wu, Y.; Gardner, S.; Ong, B. S. *Adv. Mater*. **2005**, *17*, 849−853.
(13) Meng, H.; Sun, F.; Goldfinger, M. B.; Jaycox, G. D.; Li, Z.; Marshall, W. J.; Blackman, G. S. *J. Am. Chem. Soc.* **2005**, *127*, 2406−2407.

 10.1021/ja057641k CCC: $33.50

Chart 1. Selenophene-Based Organic Semiconductors

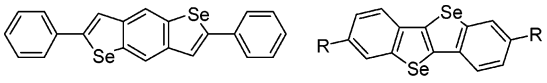

DPh-BDS

R = H BSBS (**1a**)
R = Ph DPh-BSBS(**1b**)

in the fabrication or operation of OFETs. Since most of the *p*-channel semiconductors have relatively high-lying energy levels for the highest occupied molecular orbitals (HOMOs) and relatively low excitation gaps to the lowest unoccupied molecular orbitals (LUMOs), they tend to be readily photo- or thermo-oxidizable, leading to the degradation of the resulting OFETs under ambient conditions. When processed in an inert atmosphere, regioregular poly(3-hexylthiophene)-based FET devices exhibited higher mobilities and larger current on/off ratios than those in ambient conditions.[7] The annealing of fabricated FET devices based on poly(3,3‴-dialkylquaterthiophene) and poly(3′,4′-dialkyl-2,2′:5′,2″-terthiophene) films resulted in not only high mobilities but also increased stability against oxidative doping by atmospheric oxygen.[10] Furthermore, 2,5′-bis(2-fluorenyl)bithiophenes,[11] 5,11-diarylindolo[3,2-*b*]carbazoles,[12] 2,6-bis(5-hexylthiophen-2-yl)anthracene,[13] and 5,5′-bis(2-anthracenyl)-2,2′-bithiophene[6c] were recently reported to be high-performance OFET materials with reasonable stability during operation under ambient conditions. However, there are still very few organic semiconductors endowed with both high environmental stability and high OFET performance. In our search for such organic semiconductors, we found recently that 2,6-diphenylbenzo[1,2-*b*:4,5-*b*′]diselenophene (DPh-BDS) behaves as a high-performance FET material.[14] In this system, the selenium atoms of DPh-BDS act to enhance intermolecular overlapping in the solid state, thereby facilitating charge carrier migration. As another novel potential semiconductor, we have focused our efforts on 2,7-diphenyl[1]benzoselenopheno[3,2-*b*][1]benzoselenophene (DPh-BSBS, **1b**) because of its structural similarity to DPh-BDS. Whereas the parent BSBS (**1a**) is long known,[15,16] the diphenyl derivative (**1b**) remains unknown. In this article, we report a newly developed synthetic approach to BSBS (**1a**) and DPh-BSBS (**1b**) (Chart 1) and the excellent field-effect characteristics as well as high environmental stability of **1b**-based FET devices.

Results and Discussion

MO Calculations. A number of effects are important to carrier transport in thin films of semiconducting molecules at both molecular and intermolecular levels.[17] Although it is very difficult to predict such intermolecular effects as molecular packing and phonon energies from a molecular structure itself, we considered that polycyclic heteroaromatics with large orbital coefficients on heteroatoms are especially promising as organic semiconductors, because such molecules can enhance the overlapping of frontier molecular orbitals between adjacent molecules through strong heteroatomic interactions. To obtain insight into the selenium effect of BSBS (**1a**) and DPh-BSBS (**1b**), we first carried out MO calculations by the DFT method at the B3LYP-6-31G(d) level using the PCGAMESS program.[18] The HOMO and LUMO energy levels of **1a** and **1b** are summarized in Table 1, together with those of two selenophene-based *p*-type semiconductors previously studied, DPh-BDS[14] and α-quaterselenophene (α-4S, Chart 2),[19] for comparison. Table 1 indicates that **1a** and **1b** have lower HOMO energy levels and larger HOMO−LUMO gaps than α-4S and DPh-BDS. Although lowering of the HOMO levels may be disadvantageous to charge carrier injection, the MO calculations suggest that **1a** and **1b** can behave as air-stable semiconductors. In addition, it should be noted that the four selenium-containing molecules have quite different orbital coefficients on selenium atoms in the HOMOs, as depicted in Figure 1. In the HOMO of α-4S, there are virtually no coefficients on selenium atoms, well explaining the fact that α-4S-based OFETs showed relatively low hole mobility (10^{-3} cm^2 V^{-1} s^{-1}),[19] comparable to that of α-quaterthiophene.[20] In contrast, the HOMO of DPh-BDS has large coefficients on selenium atoms, suggesting the effective contribution of polarizable selenium atoms to the intermolecular interactions for charge migration. Actually, this assumption was corroborated by the fact that FET devices made of DPh-BDS showed higher hole mobility (0.17 cm^2 V^{-1} s^{-1}) than that observed for the sulfur counterpart, 2,6-diphenylbenzo[1,2-*b*:4,5-*b*′]dithiophene (0.08 cm^2 V^{-1} s^{-1}).[14] The HOMOs of **1a** and **1b**, similar to that of DPh-BDS, have large coefficients on selenium atoms. From this result, we expected that **1a** and **1b** can function as high-performance *p*-channel semiconductors.

Table 1. Calculated HOMO and LUMO Levels[a] and HOMO−LUMO Gaps[b]

compound	HOMO/eV	LUMO/eV	Δ*E*/eV
α-4S	−4.93	−2.05	2.88
DPh-BDS	−5.21	−1.73	3.48
1a	−5.46	−1.26	4.20
1b	−5.38	−1.52	3.86

[a] Calculated at the B3LYP/6-31G(d) level. [b] Defined as |HOMO − LUMO|.

Chart 2. Structure of α-Quaterselenophene (α-4S)

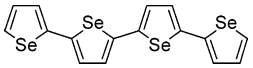

Synthesis. In 1972, Faller and Mantovani reported the first synthesis of BSBS (**1a**) as only a byproduct upon treating inaccessible *o*-methylselenobenzaldehyde with bromoacetic acid.[15] Much later, in 1988, Sashida and Yasuike reported that **1a** was obtained in 52% yield by successive one-pot reactions

(14) (a) Takimiya, K.; Kunugi, Y.; Konda, Y.; Niihara, N.; Otsubo, T. *J. Am. Chem. Soc.* **2004**, *126*, 5084−5085. (b) Zeis, R.; Kloc, C.; Takimiya, K.; Kunugi, Y.; Konda, Y.; Niihara, N.; Otsubo, T. *Jpn. J. Appl. Phys. Part 1* **2005**, *44*, 3712−3714.
(15) Faller, P.; Mantovani, F. *Bull. Soc. Chim. Fr.* **1972**, 1643−1645.
(16) Sashida, H.; Yasuike, S. *J. Heterocycl. Chem.* **1988**, *35*, 725−726.
(17) (a) Cornil, J.; Beljonne, D.; Calbert, J.-P.; Brédas, J.-L. *Adv. Mater.* **2001**, *13*, 1053−1066. (b) Brédas, J.-L.; Calbert, J. P.; da Silva Filho, D. A.; Cornil, J. *Proc. Natl. Acad. Sci. U.S.A.* **2002**, *99*, 5804−5809. (c) Brédas, J.-L.; Beljonne, D.; Coropceanu, V.; Jérôme, C. *Chem. Rev.* **2004**, *104*, 4971−5003. (d) Newman, C. R.; Frisbie, C. D.; da Silva Filho, D. A.; Brédas, J.-L.; Ewbank, P. C.; Mann, K. R. *Chem. Mater.* **2004**, *16*, 4436−4451.
(18) MO calculations were carried out by DFT methods at the B3LYP-6-31G(d) level using the PC GAMESS program. (a) Granovsky, A. A., http://classic.chem.msu.su/gran/gamess/index.html. (b) Schmidt, M. W.; Baldridge, K. K.; Boatz, J. A.; Elbert, S. T.; Gordon, M. S.; Jensen, J. J.; Koseki, S.; Matsunaga, N.; Nguyen, K. A.; Su, S.; Windus, T. L.; Dupuis, M.; Montgomery, J. A. *J. Comput. Chem.* **1993**, *14*, 1347−1363. See Supporting Information for details.
(19) Kunugi, Y.; Takimiya, K.; Yamane, K.; Yamashita, K.; Aso, Y.; Otsubo, T. *Chem. Mater.* **2003**, *15*, 6−7.
(20) (a) Katz, H. E.; Torsi, L.; Dodabalapur, A. *Chem. Mater.* **1995**, *7*, 2235−2237. (b) Hajlaoui, R.; Horowitz, G.; Garnier, F.; Arce-Brouchet, A.; Laigre, L.; Kassmi, A. E.; Demanze, F.; Kouki, F. *Adv. Mater.* **1997**, *9*, 389−391.

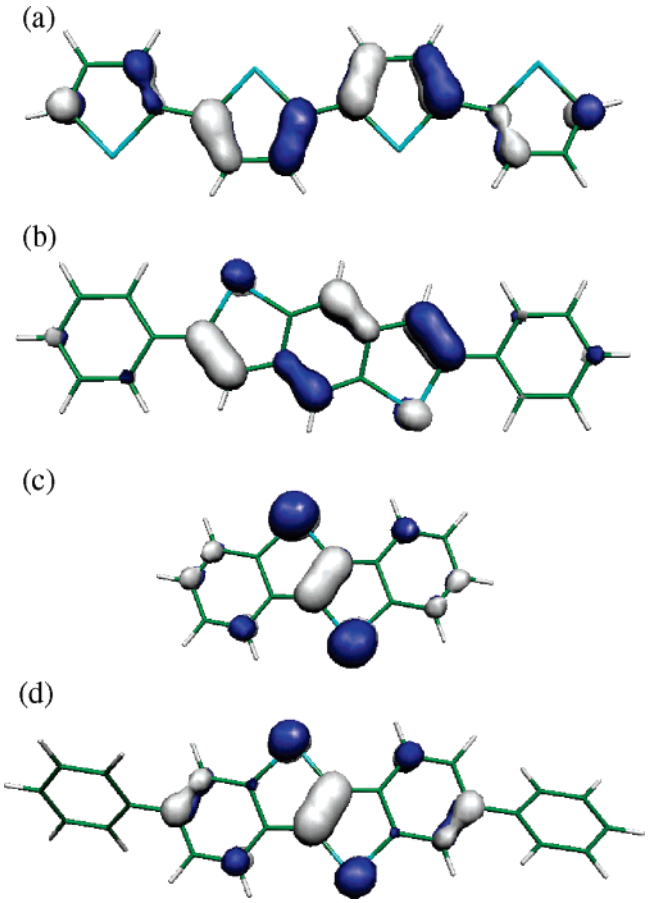

Figure 1. HOMOs of (a) α-4S, (b) DPh-BDS, (c) BSBS (**1a**), and (d) DPh-BSBS (**1b**) at the B3LYP/6-31G(d) level.

of *o*,*o*′-dibromodiphenylacetylene with *tert*-butyllithium and then with elemental selenium.[16] This method for synthetis of **1a** is quite straightforward and looks attractive; however, considering that the starting bis(3-bromobiphenyl-4-yl)acetylene is still unknown and hardly accessible, we thought that the application of the Sashida method to the synthesis of DPh-BSBS (**1b**) would be impractical. Since the Sashida reaction proceeds via *o*,*o*′-dilithiodiphenylacetylene, we first examined the generation of the same metalated species (to be exact, *o*,*o*′-dilithio(potassio)-diphenylacetylene) by direct metalation of commercially available diphenylacetylene with the LICKOR superbase (BuLi/*t*-BuOK) according to the protocol of Kowalik and Tolbert.[21] Successive treatment of the reaction mixture with selenium powder allowed for the isolation of **1a** in 28% yield, which is nearly half the yield obtained in the Sashida reaction. We then attempted the synthesis of **1b** by a similar treatment of readily available bis(biphenyl-4-yl)acetylene (**2b**),[22] but the reaction gave only a complex mixture. This forced us to develop an alternative synthetic method for the BSBS framework, as follows. The mixture obtained by reacting diphenylacetylene with the LICKOR superbase followed by selenium powder was quenched with methyl iodide to afford *o*,*o*′-bis(methylseleno)-diphenylacetylene (**3a**) in 68% yield. Subsequently, refluxing the chloroform solution of **3a** in the presence of excess iodine

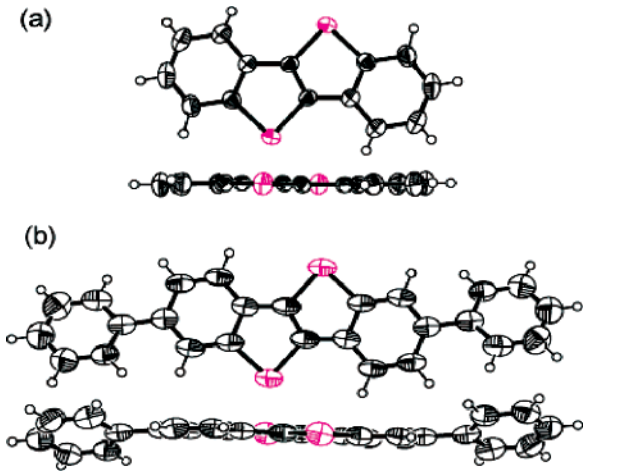

Figure 2. Molecular structures of (a) **1a** and (b) **1b**. The molecular lengths, which are defined as the distance between edge hydrogen atoms, are 10.4 and 19.0 Å for **1a** and **1b**, respectively.

Scheme 1. Synthesis of **1a** and **1b**

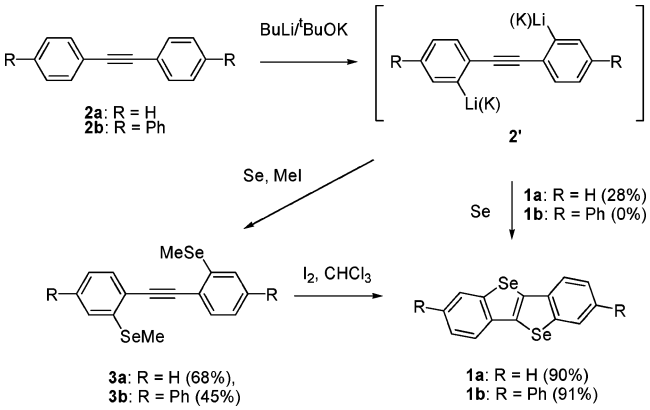

allowed for ring formation to give **1a** in 90% isolated yield after purification by column chromatography. This approach turned out to be also effective for the synthesis of diphenyl derivative **1b** via bis(3-methylselenobiphenyl-4-yl)acetylene (**3b**) from **2b** (Scheme 1).

Molecular and Crystal Structures. **1a** and **1b** were fully characterized by spectroscopic and elemental analyses. Single-crystal X-ray analyses revealed the exact molecular structures of **1a** and **1b**, where the BSBS cores are almost planar, with the maximum deviation from the mean plane being ca. 0.03 Å for **1a** and ca. 0.05 Å for **1b** (Figure 2). The attached phenyl rings in **1b** are twisted out of the central plane with a torsion angle of ca. 30°. The crystal structures of **1a** and **1b** are characterized by the "layer-by-layer" stacking mode (Figure 3). In both crystals, the unit cell contains two layers along the *a*-axis, and the molecular arrangement in each layer is classified as a herringbone type, common for crystal structures of excellent organic semiconductors such as pentacene,[23] α-sexithiophene,[24] and tetramethylpentacene.[25] In the layer of **1a**, the molecules are stacked nearly upright, and very short Se−Se contacts (3.76

(21) Kowalik, J.; Tolbert, L. M. *J. Org. Chem.* **2001**, *66*, 3229−3231.
(22) (a) Nakasuji, K.; Akiyama, S.; Nakagawa, M. *Bull. Chem. Soc. Jpn.* **1972**, *45*, 883−891. (b) Mio, M. J.; Kopel, L. C.; Braun, J. B.; Gadzikwa, T. L.; Hull, K. L.; Brisbois, R. G.; Markworth, C. J.; Grieco, P. A. *Org. Lett.* **2002**, *4*, 3199−3202.
(23) Cornil, J.; Calbert, J.-P.; Brédas, J.-L. *J. Am. Chem. Soc.* **2001**, *123*, 1250−1251.
(24) (a) Horowiz, G.; Bachet, B.; Yassar, A.; Lang, P.; Demanze, F.; Fave, J. L.; Garnier, F. *Chem. Mater.* **1995**, *7*, 1337−1341. (b) Siegrist, T.; Fleming, R. M.; Haddon, R. C.; Laudise, R. A.; Lovinger, A. J.; Katz, H. E.; Bridenbaugh, P.; Davis, D. D. *J. Mater. Res.* **1995**, *10*, 2170−2173.
(25) Meng, H.; Bendikov, M.; Mitchell, G.; Helgeson, R.; Wudl, F.; Bao, Z.; Siegrist, T.; Kloc, C.; Chen, C. H. *Adv. Mater.* **2003**, *15*, 1090−1093.

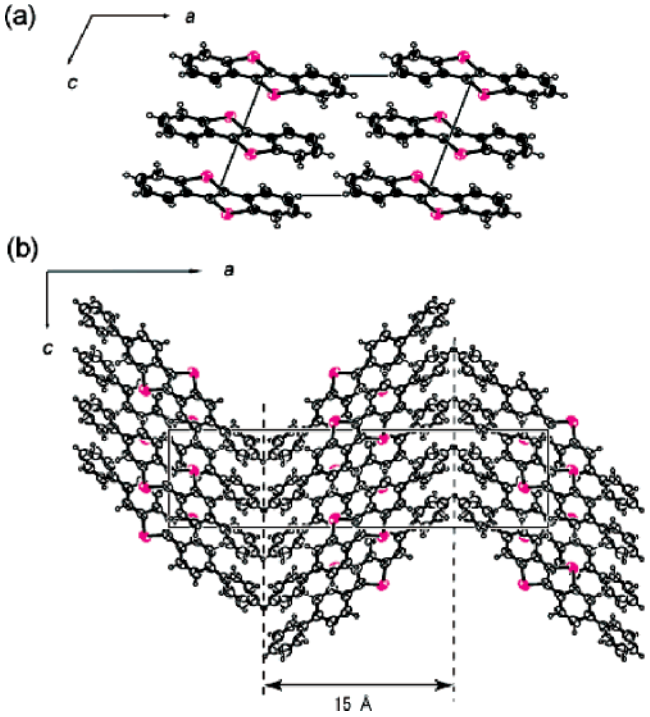

Figure 3. Crystal structures of (a) **1a** and (b) **1b**.

Å) exist. In contrast, in the layer of **1b**, the molecules are stacked with large slipping in the molecular long-axis direction. This loose packing is responsible for the layer width of ca. 15 Å and increases the Se−Se distance to 4.53 Å, meaning no selenium interaction.

Voltammetric Properties. Cyclic voltammetry of **1a** and **1b** showed irreversible oxidation waves (for the charts, see Figure S1, Supporting Information). The oxidation peaks of **1a** and **1b** were found at +1.06 and +0.86 V (vs Fc/Fc^+), respectively, which were much higher than the potentials of α-4S (+0.41 V) and DPh-BDS (+0.80 V), as expected by their calculations. On the premise that the energy level of Fc/Fc^+ is 4.8 eV below the vacuum level,[26] the HOMO levels of **1a** and **1b** were estimated using the oxidation onsets (+0.80 V for **1a** and +0.74 V for **1b**) to be 5.60 and 5.54 eV, respectively. These values are fairly consistent with the respective calculated HOMO energy levels (5.46 eV for **1a** and 5.38 eV for **1b**).

Thin Films. Parent BSBS **1a** formed no continuous thin film with good quality by thermal evaporation, because of its high crystallinity. In contrast, **1b** was readily obtained as a good thin film not only on a glass substrate but also on an *n*-doped Si wafer with 200 nm thermally grown SiO_2. The UV−vis absorption spectrum of **1b** in THF exhibited a structured $\pi-\pi^*$ band at 343 nm, as shown in Figure 4. In contrast, the absorption band of **1b** in the film phase was markedly red-shifted to 398 nm. In addition, it is remarkable that the 0−0 transition of the longest wavelength band in the film spectrum was markedly intensified to the strongest peak, in contrast to that in the solution spectrum. This observation suggests that **1b** adopts a strongly interactive stacked structure in the film phase. Presumably, the stacked structure of **1b** in the film phase is fairly tight, different

(26) (a) Brédas, J.-L.; Silbey, R.; Boudreaux, D. S.; Chance, R. R. *J. Am. Chem. Soc.* **1983**, *105*, 6555−6559. (b) Pommerehne, J.; Vestweber, H.; Guss, W.; Mark, R. F.; Bässler, H.; Porsch, M.; Daub, J. *Adv. Mater.* **1995**, *7*, 551−554.

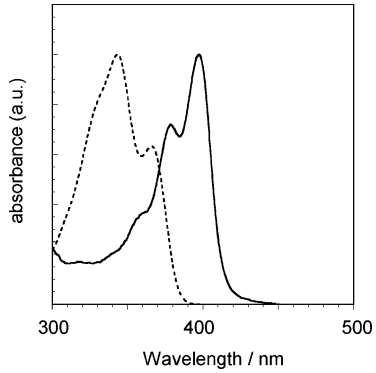

Figure 4. UV−vis spectra of **1b** in thin film (solid line) and in THF solution (dotted line).

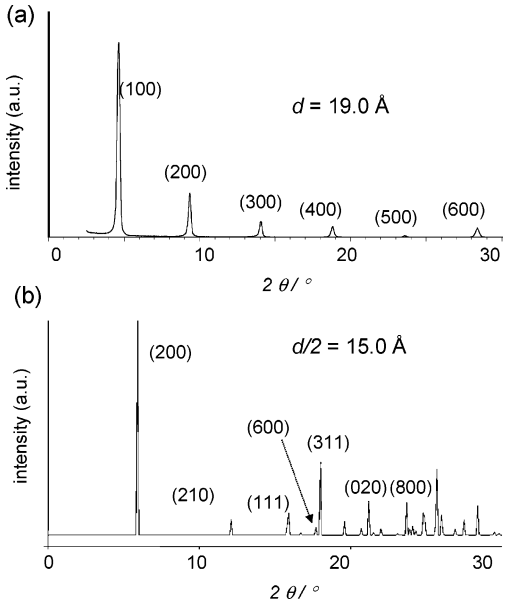

Figure 5. (a) XRD pattern of evaporated thin film of **1b** (T_{sub} = 60 °C) and (b) simulated powder pattern based on the single-crystal X-ray structure of **1b**.

from the loosely stacked structure determined by the above X-ray crystallographic analysis. The optical band gap of the thin film estimated from the absorption edge is ca. 3.0 eV, which is fairly large compared with those of typical organic semiconductors utilized for OFETs.[2−6]

To obtain further information on the film structure, the thin film of **1b** was examined by X-ray diffraction (XRD), which showed a series of peaks assignable to multiple (*h*00) diffractions, meaning that the film has a highly ordered structure (Figure 5a). On the basis of the diffraction pattern, the monolayer thickness (*d*-spacing) was determined to be 19 Å, which corresponds well to the molecular length of **1b** determined by X-ray crystallographic analysis. From this result as well as the above electronic absorption spectra, we conclude that the molecules of **1b** in the film phase are nearly perpendicular to the substrate and are aligned with close interactions. A comparison of the XRD diffraction pattern with a powder pattern simulated from the single-crystal analysis of **1b** (Figure 5b) also supports the finding that the molecular arrangement of **1b** in the film phase is different from that in the crystal phase. The tight stacking structure can increase not only π-overlapping but also Se−Se contacts between the stacked molecules, allowing for the effective contribution of polarizable selenium atoms to

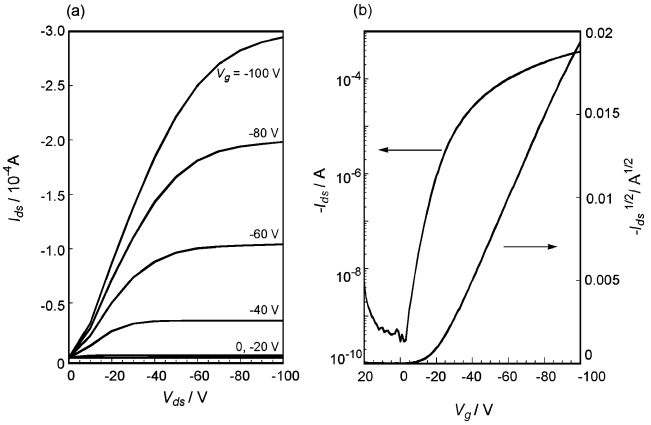

Figure 6. (a) $I_{ds}-V_{ds}$ plots as a function of V_g. (b) I_{ds} and $I_{ds}^{1/2}$ versus V_g plots at $V_{ds} = -100$ V ($T_{sub} = 60$ °C).

Table 2. FET Characteristics of DPh-BSBS-Based Devices

T_{sub}/°C	μ_{FET}/cm^2 V^{-1} s^{-1}	I_{on}/I_{off}	V_{th}/V
RT	0.19−0.20	10^6	−18
60	0.24−0.31	10^6	−20
100	0.12−0.17	5×10^5	−19

charge migration. Such a highly ordered structure in the film phase is also the case for previously studied DPh-BDS.[14a]

OFET Devices. OFET devices using the thin film of **1b** vacuum-deposited on the Si/SiO_2 substrate at different temperatures (T_{sub})—room temperature, 60 °C, and 100 °C—showed typical *p*-channel FET characteristics. Figure 6 demonstrates the FET characteristics of the device fabricated at $T_{sub} = 60$ °C: a high mobility of 0.24−0.31 cm^2 V^{-1} s^{-1} and a large current on/off ratio of 10^6 were obtained. The FET performances of the other devices fabricated at T_{sub} = room temperature and 100 °C are shown in Figure S2 (Supporting Information). As summarized in Table 2, the FET characteristics of these devices vary slightly with T_{sub}. Atomic force microscopy (AFM) images showed essentially no significant differences among the surface morphologies of the three films (Figure S3, Supporting Information).

It is emphasized that the high performance of **1b**-based OFET was maintained even when the device was operated in the presence of air and light. Figure 7 demonstrates a continuous operation test in air with repeated scanning of V_g between +20 and −100 V at constant $V_d = -100$ V. Although there was a slight shift of the threshold voltage (V_{th}) after 2000 continuous scans, there were no significant changes in mobility and I_{on}/I_{off}, even after 3000 continuous scans, indicating that **1b** is a very stable organic semiconductor. In addition, the device showed almost no deterioration in both mobility and current on/off ratio, even after it was stored under ambient laboratory conditions for more than one year (Figure S4, Supporting Information). This durability term exceeds the previously reported two months for 2,5′-bis(2-fluorenyl)bithiophenes[11] and is comparable to the very recently reported best records for 5,11-diarylindolo[3,2-*b*]carbazoles (more than one year)[12] and 2,6-bis(5-hexylthiophen-2-yl)anthracene (15 months).[13]

In summary, we have succeeded in the facile synthesis of DPh-BSBS (**1b**) by developing a straightforward selenocyclization method from bis(biphenyl-4-yl)acetylene. The thin-film devices fabricated on the basis of **1b** showed excellent *p*-type FET performances, with hole mobilities of ∼0.3 cm^2 V^{-1} s^{-1} and large current on/off ratios of $\sim 10^6$. In addition, the devices are highly durable, undergoing no significant deterioration under long-term continuous operation and during long-term storage of at least 12 months under ambient laboratory conditions. This high stability is speculated to arise primarily from the elevated oxidation potential and the increased HOMO−LUMO energy gap inherent in DPh-BSBS (**1b**). Thus, it can be concluded that DPh-BSBS is a valuable semiconducting material for practical applications and that the present successful development of DPh-BSBS supports the validity of molecular designs based on fused selenophenes in the search for air- and light-stable novel organic semiconductors.

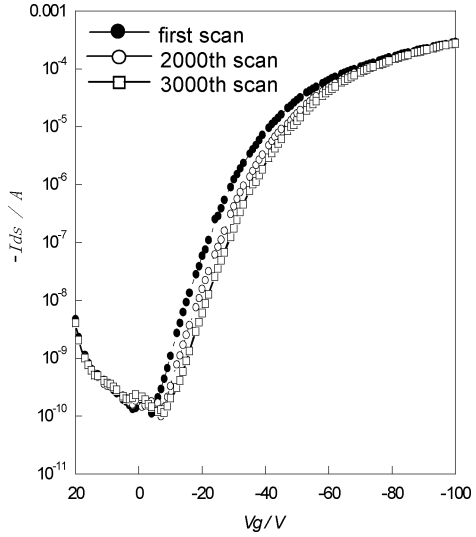

Figure 7. I_{ds} versus V_g plots at $V_{ds} = -100$ V ($T_{sub} = 60$ °C); first, 2000th, and 3000th scans.

Experimental Section

Synthesis. All chemicals and solvents were of reagent grade unless otherwise indicated. All reactions were carried out under nitrogen atmosphere. THF was purified by distillation from sodium benzophenone ketyl under nitrogen prior to use. Column chromatography was carried out with silica gel (Daisogel IR-60, 63−210 μm). Melting points are uncorrected. Nuclear magnetic resonance spectra were obtained in deuterated chloroform with a JEOL Lambda 400 spectrometer operating at 400 MHz for ^{1}H and 100 MHz for ^{13}C with TMS as internal reference; chemical shifts (δ) are reported in parts per million. EI-MS spectra were obtained on a Shimadzu QP-5050A spectrometer using an electron impact ionization procedure (70 eV). The molecular ion peaks of the selenium-containing compounds showed a typical isotopic pattern, and all the mass peaks are based on ^{80}Se. Cyclic voltammograms (CVs) were recorded on a Hokuto Denko HA-301 potentiostat and a Hokuto Denko HB-104 function generator in benzonitrile containing tetrabutylammonium hexafluorophosphate (Bu_4NPF_6, 0.1 M) as supporting electrolyte at a scan rate of 100 mV/s. Counter and working electrodes were made of Pt, and the reference electrode was Ag/AgCl. All the potentials were calibrated with the standard ferrocene/ferrocenium redox couple ($E^{1/2} = +0.46$ V measured under identical conditions). UV−vis spectra in THF solution or thin films were recorded on a Shimadzu UV-3100 spectrometer.

Bis(2-methylselenophenyl)acetylene (3a). To a suspension of *t*-BuOK (0.8 g, 7.3 mmol) in THF (15 mL) was slowly added butyllithium (1.59 M in hexane, 4.6 mL, 7.3 mmol) at −78 °C, and the resulting mixture was stirred for 20 min at the same temperature. A solution of diphenylacetylene (0.5 g, 2.8 mmol) in THF (10 mL) was added to the solution, and the mixture was stirred for another 40 min at −78 °C and then at −25 °C for 1.5 h. Selenium powder (0.44

g, 5.6 mmol) was added in several portions to the mixture at −78 °C, and the resulting mixture was stirred for 40 min at −78 °C. Methyl iodide (0.37 mL, 5.7 mmol) was then added, and the mixture was allowed to warm to room temperature. Insoluble precipitate in the reaction mixture was filtered off, and the filtrate was extracted with chloroform (20 mL × 2). The combined extracts were washed with water (20 mL) and dried ($MgSO_4$). After evaporation of the solvent, the crude product was subjected to column chromatography on silica gel eluted with dichloromethane−hexane (1:3, v/v). The desired product was obtained from the eluent of $R_f = 0.4$ and further purified by recrystallization from chloroform to give colorless needles (0.69 g, 68%): mp 108−110 °C; ^{1}H NMR ($CDCl_3$) δ 7.53 (dd, $J = 1.2$ Hz, 7.6 Hz, 2H), 7.29 (dd, $J = 1.2$ Hz, 7.6 Hz, 2H), 7.26 (dt, $J = 1.2$ Hz, 7.6 Hz, 2H), 7.17 (dt, $J = 1.2$ Hz, 7.6 Hz, 2H), 2.37 (s, 6H); ^{13}C NMR ($CDCl_3$) δ 136.18, 132.47, 128.85, 127.29, 125.02, 123.32, 93.15, 6.14; MS (EI, 70 eV) $m/z = 366$ (M^+), 351 ($M^+ - CH_3$), 336 ($M^+ - 2 \times CH_3$). Anal. Calcd for $C_{16}H_{14}Se_2$: C, 52.76; H, 3.87. Found: C, 52.75; H, 3.81.

[1]Benzoselenopheno[3,2-*b*][1]benzoselenophene (BSBS, 1a). To a solution of **3a** (0.5 g, 1.4 mmol) in refluxing chloroform (20 mL) was added powdered iodine (5.7 g, 22.4 mmol), and the resulting mixture was further refluxed for 12 h. After cooling, the solution was washed with aqueous saturated sodium sulfate solution (20 mL × 2) and water (20 mL × 2), and the chloroform layer was dried ($MgSO_4$). Evaporation of the solvent gave a yellow solid that was subjected to column chromatography on silica gel eluted with hexane−dichloromethane (3:1, v/v) to give pure BSBS (**1a**, $R_f = 0.6$) as a white solid (0.42 g, 90%). Recrystallization from chloroform gave colorless needles suitable for X-ray structural analysis: mp 207−209 °C (lit.[16] 207−208 °C); ^{1}H NMR ($CDCl_3$) δ 7.95 (dd, $J = 0.8$ Hz, 8.0 Hz, 2H), 7.79 (dd, $J = 0.8$ Hz, 8.0 Hz, 2H), 7.44 (dt, $J = 0.8$ Hz, 8.0 Hz, 2H), 7.32 (dt, $J = 0.8$ Hz, 8.0 Hz, 2H); ^{13}C NMR ($CDCl_3$) δ 141.27, 137.81, 134.28, 126.80, 125.38, 125.13, 123.84; MS (EI, 70 eV) $m/z = 336$ (M^+); CV, $E_{pa} = +1.06$ V vs Fc/Fc^+; UV−vis (THF) λ_{max} (ϵ) = 261 (24 875), 314 (25 532), 300 (21 368), 314 (25 532), 343 (11 260) nm.

Bis(biphenyl-4-yl)acetylene (2b). To a deaerated solution of 4-bromobiphenyl (5.0 g, 20 mmol) in diisopropylamine (40 mL) and dry benzene (20 mL) were consecutively added trimethylsilylacetylene (1.4 mL, 10 mmol), $PdCl_2(PPh_3)_2$ (0.84 g, 1.2 mmol), CuI (0.38 g, 2.0 mmol), DBU (1.83 g, 0.84 mmol), and water (0.14 mL, 7.8 mmol), and the resulting mixture was stirred for 18 h at 60 °C. After cooling, the mixture was diluted with water (50 mL) to precipitate a solid that was collected by filtration and washed successively with water, methanol, and hot hexane. The crude product was recrystallized from carbon disulfide to give colorless plates (1.01 g, 31%): mp 256−258 °C (lit.[22a] 253−254 °C); ^{1}H NMR ($CDCl_3$) δ 7.64−7.59 (m, 12H), 7.46 (t, $J = 7.6$ Hz, 4H) 7.44 (tt, $J = 1.2$ Hz, $J = 7.6$ Hz, 2H); ^{13}C NMR ($CDCl_3$) δ 140.97, 140.34, 132.02, 128.86, 127.63, 127.02 (× 2), 122.19, 89.98; MS (EI, 70 eV) $m/z = 330$ (M^+).

Bis(3-methylselenobiphenyl-4-yl)acetylene (3b). To a mixture of *t*-BuOK (0.89 g, 8.0 mmol) in THF (15 mL) was slowly added butyllithium (1.54 M in hexane, 5.1 mL, 8.0 mmol) at −78 °C, and the resulting mixture was stirred for 10 min at the same temperature. Bis(biphenyl-4-yl)acetylene (**2b**, 1.0 g, 3.0 mmol) was then added, and the resulting mixture was stirred for 30 min at −78 °C and then at −30 °C for 3 h. To the mixture cooled at −78 °C was slowly added selenium powder (0.47 g, 6.0 mmol) over 10 min, and the mixture was stirred at −78 °C and gradually warmed to −20 °C over a period of 4 h. At this temperature, methyl iodide (0.5 mL, 8.0 mmol) was added, and the mixture was gradually warmed over the period of 10 h. The starting material that precipitated from the mixture was removed by filtration (0.6 g, 60%), and the filtrate was extracted with chloroform (20 mL × 3). The combined extracts were washed with water (30 mL × 3), dried ($MgSO_4$), and concentrated in vacuo. The residue was subjected to column chromatography on silica gel eluted with carbon disulfide to give crude **3b** ($R_f = 0.3$) as a yellow solid. Recrystallization from chloroform gave **3b** as yellow needles (0.28 g, 18%, conversion yield 45%): mp 165−167 °C; ^{1}H NMR ($CDCl_3$) δ 7.62 (d, $J = 8.0$ Hz, 2H), 7.61−7.57 (m, 4H), 7.52 (d, $J = 1.2$ Hz, 2H), 7.47 (t, $J = 7.2$ Hz, 4H), 7.40 (dd, $J = 1.2$ Hz, 8.0 Hz, 2H), 7.39 (t, $J = 7.2$ Hz, 2H), 2.45 (s, 6H); ^{13}C NMR ($CDCl_3$) δ 141.86, 140.32, 136.66, 132.92, 128.89, 127.82, 127.13, 126.28, 124.24, 122.54, 93.84, 6.49; MS (EI) $m/z = 518$ (M^+), 503 ($M^+ - CH_3$), 488 ($M^+ - 2 \times CH_3$). Anal. Calcd for $C_{28}H_{22}Se_2(CHCl_3)_{0.5}$: C, 59.42; H, 3.94. Found: C, 59.21; H, 3.70.

2,7-Diphenyl[1]benzoselenopheno[3,2-*b*][1]benzoselenophene (DPh-BSBS, 1b). To a solution of **3b** (0.9 g, 1.7 mmol) in refluxing chloroform (20 mL) was added powdery iodine (6.9 g, 27 mmol), and the resulting mixture was further refluxed for 12 h. After cooling, the resulting solid was successively washed with aqueous saturated sodium sulfate solution (20 mL × 2), methanol (20 mL), and hot hexane (20 mL) to give **1b** as a white solid (0.75 g, 91%). Recrystallization from chlorobenzene gave an analytically pure sample as colorless plates. For device fabrication, the recrystallized sample was further purified by gradient sublimation at 320 °C (source temperature) under vacuum (10^{-3} Pa): mp > 300 °C; ^{1}H NMR ($CDCl_3$) δ 8.14 (d, $J = 1.5$ Hz, 2H), 7.83 (d, $J = 8.3$ Hz, 2H), 7.65−7.68 (m, 6H), 7.46 (t, $J = 7.6$ Hz, 4H), 7.36 (t, $J = 7.6$ Hz, 2H); MS (EI, 70 eV) $m/z = 488$ (M^+); CV, $E_{pa} = +0.86$, +1.33 V vs Fc/Fc^+; UV−vis (THF) λ_{max} (ϵ) = 283 (13 271), 343 (39 282), 366 (24 875) nm. Anal. Calcd for $C_{26}H_{16}Se_2$: C, 64.21; H, 3.32. Found: C, 64.60; H, 3.32.

X-ray Crystallographic Analysis. A single crystal of **1a** suitable for X-ray crystallographic analysis was grown by recrystallization from chloroform, whereas that of **1b** was grown by horizontal physical vapor transport in flowing argon gas.[27] X-ray crystal structure analyses were performed on a Rigaku AFC7R four-circle diffractometer (Mo Kα radiation, $\lambda = 0.71069$ Å, graphite monochromator, $T = 296$ K, ω scan, $2\theta_{max} = 55.0°$). The structure was solved by direct methods.[28] Non-hydrogen atoms were refined anisotropically.[29] Hydrogen atoms were included but not refined. All calculations were performed using the crystallographic software package teXsan.[30] Crystal data for BSBS (**1a**): $C_{14}H_8Se_2$, $M = 334.14$, colorless plate, 0.50 × 0.20 × 0.03 mm^3, monoclinic, space group $P2_1/c$ (No. 14), $a = 12.037(2)$ Å, $b = 6.025(1)$ Å, $c = 8.420(1)$ Å, $\beta = 108.45(1)°$, $V = 579.2(2)$ Å^3, $Z = 2$, $D_{calc} = 1.916$ g cm^{-3}, $R = 0.035$ for 1083 observed reflections ($I > 2\sigma(I)$) and 85 variable parameters, $R_w = 0.111$ for all data. Crystal data for DPh-BSBS (**1b**): $C_{26}H_{16}Se_2$, $M = 486.30$, colorless plate, 0.40 × 0.20 × 0.01 mm^3, orthorhombic, space group *Pbca* (No. 61), $a = 30.008(7)$ Å, $b = 8.400(4)$ Å, $c = 7.701(3)$ Å, $V = 1940(2)$ Å^3, $Z = 4$, $D_{calc} = 1.650$ g cm^{-3}, $R = 0.043$ for 1009 observed reflections ($I > 2\sigma(I)$) and 128 variable parameters, $R_w = 0.169$ for all data.

Device Fabrication. OFETs were fabricated in a "top-contact" configuration on a heavily doped n^+-Si (100) wafer with 200-nm-thick thermally grown SiO_2 ($C_i = 1.73 \times 10^{-8}$ F cm^{-2}). A thin film (50 nm thick) of DPh-BSBS (**1b**) as the active layer was vacuum-deposited on the Si/SiO_2 substrate maintained at various temperatures (T_{sub}) at a rate of 1−2 Å s^{-1} under a pressure of ~2×10^{-3} Pa. On the top of the organic thin film, gold films (80 nm) as drain and source electrodes were deposited through a shadow mask. For a typical device, the drain−source channel length (L) and width (W) are 50 μm and 1.5 mm, respectively. The characteristics of the OFET devices were measured at room temperature under vacuum or in air with an Agilent 4155C semiconductor parameter analyzer. Field-effect mobility (μ_{FET}) was calculated in the saturation regime of the I_{ds} using the equation $I_{ds} = (WC_i/2L)\ \mu_{FET}(V_g - V_{th})^2$, where C_i is the capacitance of the SiO_2 insulator and V_g and V_{th} are the gate and threshold voltages, respectively.

(27) Laudise, R. A.; Kloc, Ch.; Simpkins, P. G.; Siegrist, T. *J. Crystal Growth* **1998**, 187, 449−454.
(28) Altomare, A.; Burla, M. C.; Camalli, M.; Cascarano, M.; Giacovazzo, C.; Guagliardi, A.; Polidori, G. *J. Appl. Crystallogr.* **1994**, *27*, 435−436.
(29) Sheldrick, G. M. *Program for the Refinement of Crystal Structures*; University of Goettingen: Goettingen, Germany, 1997.
(30) *teXsan: Single Crystal Structure Analysis Software*, Version 1.11; Molecular Structure Corporation and Rigaku Corporation, 2000.

Current on/off ratio (I_{on}/I_{off}) was determined from the I_{ds} at $V_g = 0$ V (I_{off}) and $V_g = -100$ V (I_{on}). The mobility and I_{on}/I_{off} data summarized in Table 2 are typical values obtained from several devices.

XRD and AFM Images of DPh-BSBS Film. X-ray diffraction patterns of DPh-BSBS thin films deposited on the Si/SiO_2 substrate were obtained with a Maxscience M18XHF diffractometer with a Cu Kα source ($\lambda = 1.541$ Å) in air. AFM images of DPh-BSBS thin films on Si/SiO_2 were obtained with a Shimadzu SPM-9500 microscope in air (see Figure S3 in Supporting Information).

Acknowledgment. This work was partially supported by Grants-in-Aid for Scientific Research on Priority Areas of Molecular Conductors (Nos. 15073218 and 16038219) and Scientific Research (Nos. 15550162 and 16750162) from the Ministry of Education, Culture, Sports, Science and Technology, Japan, and an Industrial Technology Research Grant Program in 2005 from the New Energy and Industrial Technology Development Organization (NEDO) of Japan. K.T. is indebted to The Furukawa Foundation for financial support. We are also grateful to Professor S. Yamanaka (Hiroshima University) for XRD measurements.

Supporting Information Available: Cyclic voltammograms of **1a** and **1b**; FET characteristics of **1b**-based OFETs fabricated at T_{sub} = room temperature and 100 °C; AFM images of thin films of **1b**; transfer characteristics of typical devices in saturated regimes as a function of time; details of DFT calculations of **1a**, **1b**, α-quaterselenophene (α-4S), and DPh-BDS. (PDF). Crystallographic information file for **1a** and **1b** (CIF). This material is available free of charge via the Internet at http://pubs.acs.org.

JA057641K